11th World Congress on Computational Mechanics (WCCM XI)
5th European Conference on Computational Mechanics (ECCM V)
6th European Conference on Computational Fluid Dynamics (ECFD VI)
E. Oñate, J. Oliver and A. Huerta (Eds)

TOWARDS A MULTI-FIDELITY APPROACH FOR CFD SIMULATIONS OF VORTEX GENERATOR ARRAYS

L. FLORENTIE*, A.H. VAN ZUIJLEN AND H. BIJL

Aerodynamics Group, Faculty of Aerospace Engineering
Delft University of Technology
Kluyverweg 2, 2629HT Delft, The Netherlands
*e-mail: l.florentie@tudelft.nl

Key words: Vortex Generators, CFD, Turbulence Modeling, Multi-Fidelity Modeling

Abstract. This paper is the starting point for the development of a multi-fidelity modeling approach for vortex generators (VG) arrays, where a fully resolved VG model will be coupled with an approximate model in order to improve both accuracy and flexibility without increasing the required computational cost. As a first step thereto, an analysis of the ability of the BAY-model to simulate incompressible flows around a VG on a flat plate has been performed. Results are presented for several turbulence models and using different cell selection approaches, where comparison is made with fully resolved VG results. In addition to a coarse uniform mesh, the BAY-model has been evaluated on a densely gridded mesh in order to distinguish between model and mesh related discrepancies.

1 INTRODUCTION

The addition of flow control devices like vortex generators (VGs) to e.g. airplane wings, wind turbines and engine inlet ducts has been proven to increase their performance considerably [1, 2, 3]. VGs are small vanes, which are mounted on a surface at an angle relative to the incoming flow. They introduce streamwise vortices into the boundary layer, thereby mixing the high-momentum flow in the outer region of the boundary layer with the low-momentum flow near the surface. This increases the energy in the lower part of the boundary layer and hence prevents (or significantly delays) flow separation from occurring. By ensuring an attached flow over a larger portion of the surface the lift forces are effectively increased, resulting in e.g. an increase in power generated by the turbine.

The growing demand for clean energy results in innovative designs and upscaling of wind turbines, hence requiring assessment and development of aerodynamic tools that are applicable for these unconventional conditions. Since passive VGs are commonly applied on turbine blades where they have a large effect on the local flow characteristics, it is therefore important to be able to accurately determine the optimum VG configurations for specific operating conditions. The latter requires the ability to accurately model and predict the physics associated with the flow patterns around individual VGs and the combined effects encountered for VG arrays. CFD methods are extremely suited for this purpose. However, due to the large difference in scale between a VG (with a height typically only a fraction of the boundary layer thickness) and the surface where it is applied, inclusion of VGs in accurate CFD simulations requires locally very dense meshes and therefore induces high computational costs.

In order to still be able to include the effects of VG arrays in flow simulations, often the effect induced by a VG is modeled rather than including the geometry itself into the mesh. To this end several techniques have been developed, the majority of which are based on the addition of a source term to the governing equations in order to enforce the formation of a vortex with the desired properties. An extensive overview of source term modeling techniques is contained in [4]. In general, distinction is made between methods that model the generated vortex profiles [5, 6, 7] and methods that model the body force generated by the VG in order to induce these profiles [8, 9, 10]. Although qualitatively accurate predictions for the downstream flow field have been obtained, in general flow subtleties due to viscous effects, turbulence and complex inflow conditions cannot be represented correctly by these simplified models. Moreover, the first category relies heavily on analytical vortex profiles (often the Lamb-Oseen model) in combination with empirical relations. The latter makes this type of modeling approaches unsuitable for accurate calculations of unconventional VG lay-outs.

In an attempt to resolve some of the issues related to the approximate VG modeling approaches described above, our current research focuses on constructing a multi-fidelity approach that combines the benefits of both fully resolved VG simulations and approximate models. A short outlook of our ideas in that direction is contained in the next section.

2 CONSTRUCTION OF A MULTI-FIDELITY APPROACH

It is assumed that an accurate representation of the boundary layer characteristics already from the initial vortex formation will improve both the accuracy and range of validity of the VG model. To this end we aim to develop a multi-fidelity approach that will be capable of improving the accuracy of approximate VG models based on local fully resolved VG results. The preliminary idea in that direction consists of constructing a reduced order or surrogate model based on the approximate model that is improved during runtime. An overview of the simulation steps that are likely to be required for such a modeling approach is contained in figure 1, where a source term method is assumed as approximate VG model. In this overview, x indicates the data that is extracted from the low-fidelity model in order to serve as input for the surrogate and high-fidelity models, that subsequently determine the correction $\tilde{y}$ to be applied to the coarse model.

In order to be efficient, of course as few as possible high-fidelity evaluations should be required. Hence, the identification of an appropriate surrogate construction and cali-

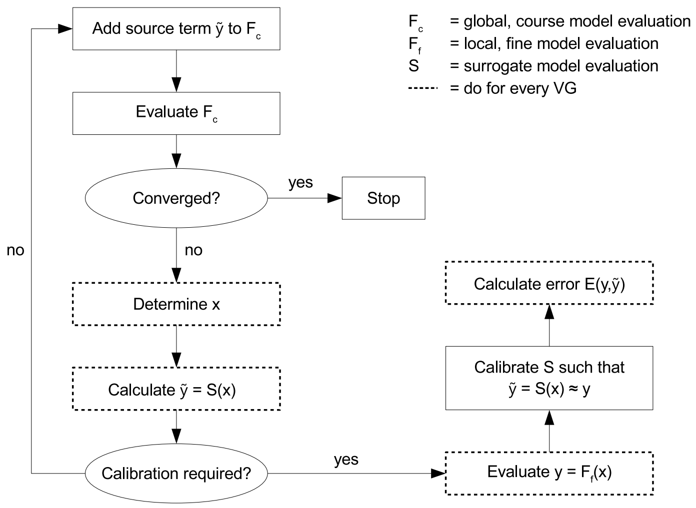

Figure 1: Overview of a possible multi-fidelity modeling approach.

bration method will be an important part of the research. Another aspect that requires investigation is the choice of appropriate low- and high-fidelity models. To this end first a closer look is taken to both suitable turbulence modeling approaches (section 4) and the commonly applied approximate VG model of Bender et al. [8]. Apart from the general performance of this model, also the mesh resolution and the selection of cells where the model is applied are considered in section 5.

3 DESCRIPTION AND IMPLEMENTATION OF THE BAY-MODEL

The BAY-model [8], developed for vane type VGs, adds a source term to the momentum and energy equations that describes the side force (lift force) induced by the VG, in order to mimic the generated flow field. By considering the VG as a thin airfoil, Joukowski's lift theorem in combination with a small angle approximation yields

$$\mathbf{L}_i = cS_{VG}\frac{V_i}{V_{tot}}\rho_i(\mathbf{u}_i \cdot \hat{\mathbf{n}})(\mathbf{u}_i \times \hat{\mathbf{b}})\left(\frac{\mathbf{u}_i}{|\mathbf{u}_i|} \cdot \hat{\mathbf{t}}\right), \tag{1}$$

for the local lift force acting in cell i, where $\mathbf{u}_i$ and ρ_i are the local flow velocity and density, S_{VG} is the surface area of the VG and $\hat{\mathbf{n}}$, $\hat{\mathbf{b}}$ and $\hat{\mathbf{t}}$ are unit vectors describing the orientation of the VG (see figure 2). The source term should be applied in those cells corresponding to the physical location of the VG, where scaling to the local cell is done by multiplication with the ratio of the current cell volume to the total volume of cells where the model is applied. Furthermore, (1) contains a constant c that controls the strength of the force and hence the intensity with which the local flow field aligns with the virtual VG. In general it is found that for values of $c > 10$ the solution becomes independent of

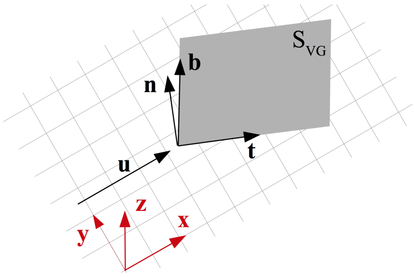

Figure 2: Illustration of the VG orientation vectors as used in (1) to calculate the lift force.

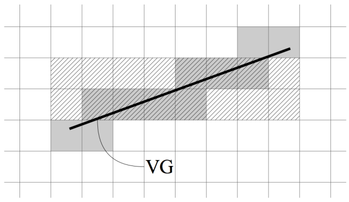

Figure 3: Top view of cells where the source term is applied: the original approach uses the striped cells, the aligned and the interpolated approaches use the grey cells.

this constant [8]. In order to make sure that our results are independent of this constant, in the current work $c = 15$ has been used.

3.1 Implementation of the BAY-model

The BAY-model has been implemented successfully in the open source CFD code OpenFOAM for an incompressible RANS solver. However, it is found that for values of $c > 1$ the disturbing effect of the source term is large and underrelaxation is required to facilitate convergence.

Our implementation of the BAY-model includes several options to distribute the source term over the grid cells, as illustrated in figure 3. First of all an intuitive *aligned* approach is used where the source term is applied in every cell that would contain part of the VG if it were to be included into the mesh, using the cell volume scaling as included in (1). Also the *original* distribution approach as proposed by Bender et al [8] is implemented. This approach consists of applying the source term in a volume of cells that span the chord of the VG, where the width of the volume is used to calibrate the total lift force. In [8] it is suggested to determine the number of rows where the model is applied by matching the normalized cross stream mean kinetic energy K, defined as

$$K = \frac{\int_A \rho(v^2 + w^2)dA}{\int_A \rho u^2 dA}. \tag{2}$$

This is an important quantity when analyzing the likelihood of the boundary layer to separate and hence an intuitive choice for calibration. The third option that is implemented is an *interpolation* method based on Jirasek's approach [10]. The lift force is calculated at the actual VG location by first determining the intersections of the (zero thickness) VG with the cell faces and by interpolation of the local velocity field to these intersection points. For the latter inverse distance weighting interpolation is used taking into account the corner points of the cells. The calculation of the intersection points also allows to determine the actual surface of the VG contained in a particular cell. The actual lift force that is included in the selected cells is therefore determined as the average of its face values, using a scaling based on the VG surface ratio. So for this interpolation approach, in (1) the term $S_{VG}V_i/V_{tot}$ is replaced by S_i.

3.2 Description of the test case

In the following, results obtained using both a fully resolved (gridded) VG simulation and the BAY-model are presented. The test case for which the results are obtained consists of a single VG on a flat plate in incompressible flow at Mach 0.1. A fully developed turbulent boundary layer is assumed, with a boundary layer thickness $\delta = 45$mm at the leading edge of the VG. This is the same test case as used by Waithe [9], hence for more details we refer to his work. The experimental data used to validate our numerical results are also taken from [9].

The mesh used for the gridded VG simulations consists of approximately 1.15 million cells with average y^+ values of 16 and 37 on the bottom plate and VG surface respectively. Since no separation occurs along the plate, for this test case wall functions are used to model the flow near the solid boundaries, hence avoiding the requirement of very fine cells with $y^+ < 1$ in these regions.

Application of an approximate source term model to simulate VG flows does not require the inclusion of the VG geometry into the computational mesh. Hence, in theory the same mesh resolution as for undisturbed wall bounded flows can be used. Therefore we used a uniform structured mesh for the BAY-model simulations with the same boundary layer resolution as used for the gridded VG simulations, so with $y^+ \approx 16$ and making use of wall functions. To be able to resolve the induced vortices, still some minimal mesh resolution is required. In lateral and streamwise direction we therefore chose to use a resolution corresponding to approximately 15% of the VG chord length. This results in a computational mesh consisting of 357000 cells, which is only 30% of the mesh size required for the gridded VG simulations.

4 TURBULENCE MODELING

As a first step we consider numerical simulations employing different turbulence models. Two closure strategies are considered for the RANS equations, being the use of linear eddy viscosity models and by solving the Reynolds stress transport (RST) equations. In particular, the following turbulence models are used:

- the one-equation Spalart Allmaras (SA) model,
- the two-equation $k - \epsilon$ model,
- Menters two-equation $k - \omega$ SST model,
- the RST model of Launder, Reece and Rodi (LRR) [11],
- and the RST model of Launder and Gibson (LG) [12].

More information about these turbulence modeling approaches can be found in [13].

The results presented in this section are obtained for the gridded VG simulation, however, very similar behavior is observed when using the BAY-model. In order to avoid duplicate figures, those results are therefore not included.

In figure 4 the primary vortex characteristics are shown in terms of the evolution of the streamwise peak vorticity, the circulation and the vortex radius. The latter is defined as half the distance between the secondary velocity peaks (as shown in figure 6 for the BAY-model). As expected, figure 4(a) shows that both RST models are most capable of accurately representing the peak vorticity close behind the VG, where especially the LG model matches the experimental data very closely for this test case. The linear eddy viscosity models, on the other hand, strongly underestimate (the two-equation models) or overestimate (the SA model) the generated vorticity.

From figure 4(b), showing the total circulation, also the different vortex decay rates of the applied turbulence models can be deduced. With exception of SA, the initial circulation close behind the VG is very similar for all models and close agreement with the experimental data is obtained. This graph clearly shows the difference between the two RST models: the wall corrections included in the LG model mainly consist of locally lowering the diffusivity of the model. The reduced dissipation rate of the LG model compared to the LRR model is also observed in figure 4(c). Moreover, it is observed that despite the poor performance in modeling ω_{max}, the two-equation eddy viscosity models, and in particular the $k-\omega$ SST model, display rather good vortex decay characteristics that resemble the experimental data. However, the failure of these models to provide reliable estimates of the turbulent viscosity results in rapid dissipation of the vortex core.

The vorticity overestimation of the SA model is also observed when looking at the total circulation, hence making the model rather unfit for accurate predictions regarding the obtained flow mixing and therefore the performance of the VG. Although the SA model is very efficient, it has clear limitations as general turbulence model making it unsuitable for representing the complex (high Re) flow characteristics that occur behind a VG. However, in this particular case the model seems to predict the growth of the vortex rather well. A close agreement with the vortex radius obtained using the accurate RST model of

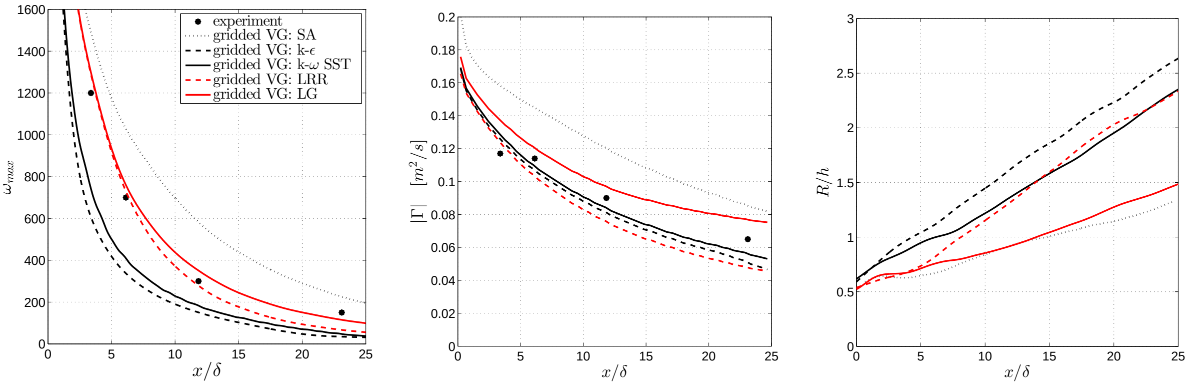

(a) Streamwise peak vorticity. (b) Circulation. (c) Growth of the vortex radius.

Figure 4: Comparison of numerical results with experimental data [9], for a gridded VG using different turbulence modeling approaches.

Launder and Gibson is perceived for the gridded VG simulations. Although not shown here, using the BAY-model on the other hand, the SA model yields an underprediction of R compared to the LG result.

Overall, the results of our VG simulations indicate that, as expected, the use of a RST closure yields the most accurate results. However, when disregarding ω_{max}, also the cheaper two-equation model of Menter behaves satisfactory. Especially the good results with respect to the total circulation and vortex decay, which are important when evaluating the mixing of the flow in the boundary layer, indicate that this model can be trusted to yield efficient yet accurate flow development predictions for the vortices as generated by micro VGs.

5 PERFORMANCE OF THE BAY MODEL FOR FLAT PLATE FLOW

The main reason to use an approximate model like the BAY-model over a fully gridded CFD simulation consists of keeping the related computational cost manageable. Hence, the need for mesh refinements should be avoided and in general coarse structured meshes are used. For the same reason such models are usually applied in combination with a computationally cheap eddy viscosity turbulence closure strategy, instead of using accurate RST models. From section 4 it followed that in this case Menters $k-\omega$ SST model is an appropriate choice, therefore this model is used to obtain the following results.

5.1 General performance and mesh dependence of the model

In order to evaluate the accuracy and efficiency of the BAY-model, it is important to distinguish between performance characteristics due to the low mesh resolution and characteristics related to the model itself. Therefore we performed simulations employing two mesh resolutions: the coarse mesh as described in section 3.2, and a fine mesh equal to the mesh used for the gridded VG simulations. In both cases the original approach (calibrated w.r.t. the gridded VG result) is used to determine the cells where the source term is added. Hence, any deviations between the BAY-model on the fine mesh and the gridded VG results are due to the VG modeling approach.

The results used to analyze the mesh dependent performance of the BAY-model are included in black in figure 5. As seen from figure 5, the BAY-model predicts the vortex development rather well, its major deficiency is the underprediction of the generated vorticity intensity. When solely looking at the streamwise peak vorticity, the model yields an average error of approximately 25% compared to the gridded VG results over a distance of 2δ (or almost 9 time the VG height) downstream of the VG. On a coarse mesh the ability to capture this peak decreases even further, yielding an underestimation of even 50%. However, due to the slightly lower vortex decay rate (as can be deduced from figure 5(b)) this error decreases with downstream distance. Although the BAY-model fails to capture ω_{max}, it performs much better when looking at the total circulation downstream of the VG. This good agreement in $|\Gamma|$ for the BAY-model is not surprising, because the

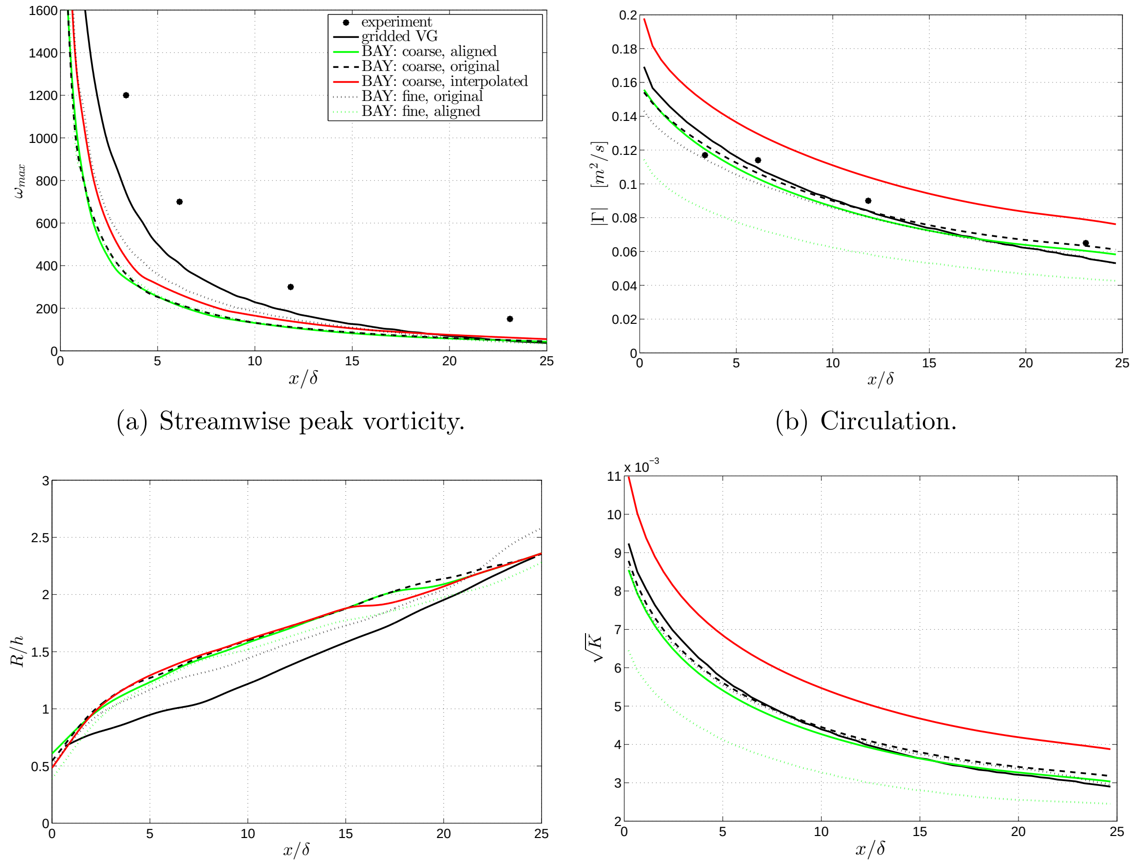

(a) Streamwise peak vorticity.

(b) Circulation.

(c) Growth of the vortex radius.

(d) Cross stream kinetic energy.

Figure 5: Comparison of the vortex characteristics obtained using the BAY-model on both a fine and a coarse mesh, using the $k-\omega$ SST turbulence model.

model has been calibrated based on the cross stream kinetic energy (defined by (2) and shown in figure 5(d)), which is closely related to Γ. Hence, for uncalibrated cell selection approaches this error increases, as discussed in section 5.2. Still, it must be noted that the fine mesh result, which has the smallest calibration error, yields a larger error w.r.t. the total circulation than does the BAY-model on a coarse mesh (an initial underprediction of 13% and 6% respectively). It is believed that this is due to the discrete integration of the vorticity, where the low resolution can cause a small overprediction of the actual result.

Furthermore, rather large discrepancies are observed with respect to the vortex radius (figure 5(c)). Even on the same mesh, the BAY-model results in an overprediction of the vortex radius compared to the fully resolved VG simulation. This is despite an initial underprediction of the quantity, since it is followed by a short period of rapid growth. Looking on a more representative coarse mesh, the overprediction of the BAY-model is even larger. Note that a cubic spline curve fitting has been used in determining the velocity peaks for these coarse mesh results. When comparing this graph with the gridded VG results for different turbulence models, it is observed that the $k - \omega$ SST model already tends to overestimate the vortex radius compared to the RST models. Hence, the performance of the BAY-model in modeling the vortex radius seems to be rather unsatisfactory.

5.2 Influence of calibration and the cell selection approach

The results obtained with the calibrated BAY-model (as discussed in section 5.1 and included in the figures in black) show that the model is able to perform satisfactory. However, calibration requires the availability of high-fidelity data, which is generally not the case. Therefore it is worthwhile to look at the results obtained using the other cell selection approaches, as introduced in section 3.1, which are also contained in figures 5(a) to 5(d). First of all it is observed that there is a large difference in results for ω_{max}, Γ and $\sqrt{K}$ depending on the cell selection approach, whereas the influence on R is very limited.

If we look at the aligned approach on the coarse mesh, it is observed that this method is calibrated equally well as the original rectangular approach. Therefore also the obtained vortex development is very similar. This indicates that selecting cells aligned with the actual location of the VG does not improve the performance of the model. Moreover, the same cell selection procedure does not yield a calibrated result on the fine mesh. Therefore this procedure does not improve the originally proposed cell selection approach, nor does it eliminate the need for calibration. Also the cell selection approach where the flow variables are interpolated to the actual VG location does not yield a well calibrated kinetic energy. This translates to the generated vortex, which deviates from the reference values with respect to both circulation and core area. Moreover, the required interpolation of flow variables adds to the computational cost of the method.

This short analysis of alternative cell selection methods highlights the importance of the calibration step when using the BAY-model to simulate VG flows. If the model is poorly calibrated the circulation and mean kinetic energy can be over- or underpredicted significantly, resulting in erroneous conclusions regarding the VG effectiveness.

5.3 Velocity profiles close to the VG

Since the differences between the BAY-model and the gridded VG simulations originate from the early vortex development phase (the downstream behavior is governed by the turbulence model), it is interesting to look at the secondary velocity profiles close behind the VG in more detail. Therefore the normalized velocities in lateral and vertical direction at several downstream locations are presented in figure 6, using the original (calibrated) cell selection approach and the $k - \omega$ SST turbulence model. In general, a very close agreement between the gridded VG results and the BAY-model (using the same mesh) is observed, especially for the U_z-profiles. The largest discrepancies are observed for U_y close to the surface. As expected, due to the low resolution the velocity peaks are less

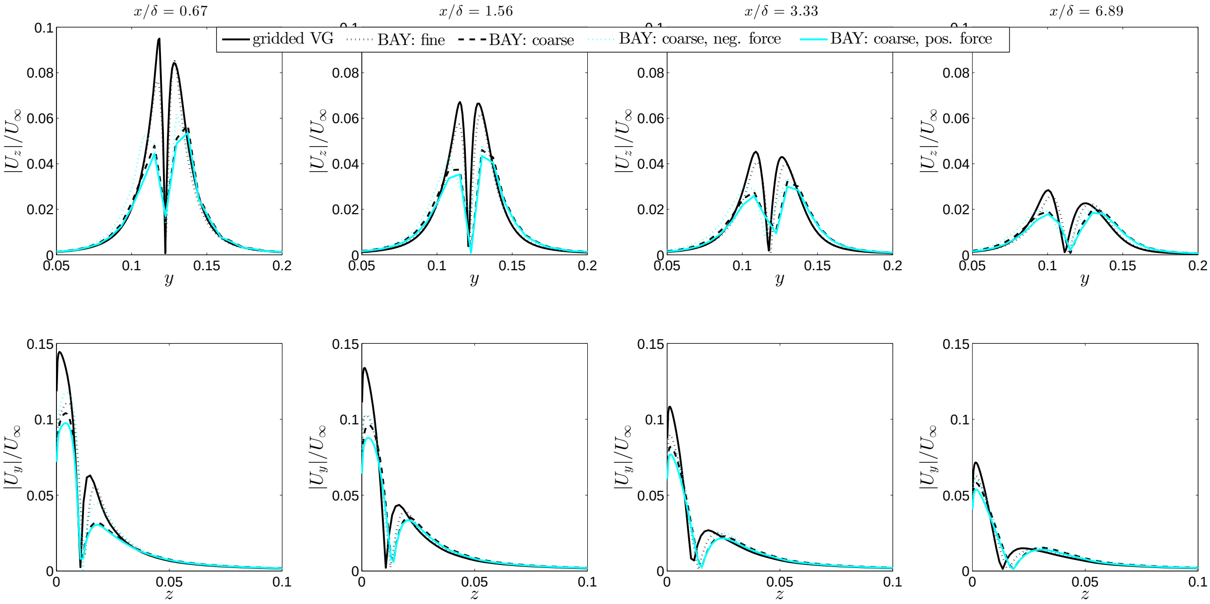

Figure 6: Normalized secondary velocity profiles (through the vortex center) for the gridded VG and the BAY-model with different mesh resolutions and additional forces in streamwise direction.

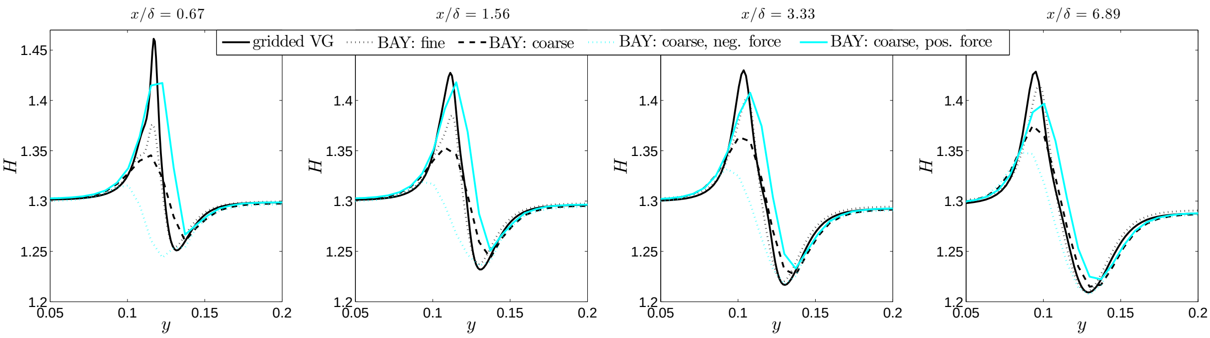

Figure 7: Boundary layer shape factor at different downstream locations for the gridded VG and BAY-model with different mesh resolutions and additional forces in streamwise direction.

pronounced for the results obtained with the BAY-model on the coarse mesh. Furthermore, these graphs indicate the location of the vortex center for the considered cases. It is observed that the initial vortex location is modeled correctly by the BAY-model. However, when moving downstream the vortex center slowly starts to deviate from the reference result, where the main deviations occur in vertical direction.

Apart from the vortex development, an accurate model is also expected to yield good predictions of the general boundary layer characteristics. Therefore it is worthwhile to have a closer look at the boundary layer shape factor,

$$H = \frac{\delta^*}{\theta} = \frac{\int_0^\infty 1 - \frac{u}{U_\infty} dz}{\int_0^\infty \frac{u}{U_\infty}(1 - \frac{u}{U_\infty}) dz}, \tag{3}$$

for both modeling approaches. This quantity is found to be barely influenced by the applied turbulence model. The VG modeling approach, on the other hand, does have an influence on H. Figure 7 shows that on a fine mesh the BAY-model is able to obtain close agreement, however, this only happens after a distance of approximately 5δ downstream. Closer to the VG the disturbing effect of the VG in streamwise direction is underestimated. When looking at the results on the coarse mesh, again a larger underestimation is observed. These figures seem to indicate that the addition of only a lateral body force is not enough to properly model the boundary layer downstream of a VG. Since we found that the addition of a small skin friction drag source term has a negative influence on the local shape factor profiles (included in figures 6 and 7 in blue and dotted), it is to be expected that changing its direction improves the results with respect to H.

Indeed, preliminary results indicate that adding a small force in streamwise direction to the model has a beneficial effect on the shape factor, while only having minor influence on the secondary velocity profiles and general vortex characteristics like Γ and ω_{max}. The addition of this force actually causes the angle of the source term w.r.t. the flow direction to be altered, such that it is no longer perpendicular to the local velocity. It is observed that tilting this vector backwards, as e.g. by the addition of a drag term, barely improves the agreement in secondary flow profiles, while having a negative influence on H. Tilting the source term forward on the other hand improves the boundary layer shape factor but slightly reduces the secondary velocity peaks. Hence, these preliminary results seem to indicate that modeling both the vortex development and the boundary layer shape correctly requires a more involved approach than simply applying a uniform body force to the governing equations.

6 CONCLUSIONS

As a first step towards the development of a multi-fidelity modeling approach for VG arrays, we looked into the performance of a commonly used approximate VG model.

An analysis of the BAY lift force model for incompressible flow over a VG on a flat plate has been presented, including different turbulence models and cell selection approaches. Although the presented results have been obtained for a single test case only and do therefore not suffice to make general statements regarding the performance of the model, they highlight some important properties and possible pitfalls.

Overall it has been observed that the model performs rather well in simulating the vortex development and evolution induced by the VG. However, this requires the model to be calibrated, which is generally not possible due to the absence of high-fidelity data. Investigated alternative cell selection methods were not able to alleviate this issue. Moreover, the low mesh resolution that is inherently related to the modeling approach causes an inability to accurately capture peaks in the velocity profiles (and hence the vorticity). Other observed deficiencies of the BAY-model for the considered test case include the overestimation of the vortex radius and inaccurate shape factor results. These issues therefore reduce the reliability of the model, especially close behind the VG.

With respect to the turbulence modeling approach it is observed that only the RST models are capable of capturing the streamwise vorticity peaks. However, the total circulation and vortex decay are predicted well by computationally less expensive two-equations models like the $k - \omega$ SST model of Menter, making it an appropriate choice for use in combination with an approximate VG model.

7 ACKNOWLEDGEMENTS

This research is part of the AVATAR project, which is initiated by the European Energy Research Alliance (EERA) and carried out under the FP7 program of the European Union.

REFERENCES

[1] Miller, G.E. *Comparative performance tests on the Mod-2 2.5MW wind turbine with and without vortex generators*. NASA TM N95-27978, 1984.

[2] Øye, S. *The effect of vortex generators on the performance of the ELKRAFT 100 kW turbine*. 9th IEA Symposium on Aerodynamics of wind turbines, 1995.

[3] Lin, J.C. *Review of research on low-profile vortex generators to control boundary layer separation*. Progress in Aerospace Sciences, Vol. 38, pp. 389-420, 2002.

[4] Booker, C. and Zhang, X. *Large-scale source term modeling of vortex generation*. AIAA2009-3951, 2009.

[5] Kunik, W.G. *Application of a computational model for vortex generators in subsonic internal flows*. AIAA-86-1458, 1986

[6] May, N.E. *A new vortex generator model for use in complex configuration CFD solvers*. AIAA...

[7] Törnblom, O. and Johansson, A.V. *A Reynolds stress closure description of separation control with vortex generators in a plane asymmetric diffuser*. Phys. Fluids, Vol. 19, No. 11, 2007

[8] Bender, E.E. , Anderson, B.H. and Yagle, P.J. *Vortex generator modeling for Navier-Stokes codes*. FEDSSM99-6919, 1999.

[9] Waithe, K.A. *Source term model for vortex generator vanes in a Navier-Stokes computer code*. AIAA2004-1236, 2004.

[10] Jirasek, A. *Vortex generator model and its application to flow control*. Journal of Aircraft, Vol. 42, No. 6, p. 1486-1492, 2005.

[11] Launder, B.E., Reece, G.J. and Rodi, W. *Progress in the development of a Reynolds-stress turbulence closure*. J. Fluid Mech., Vol. 68(03), pp. 537-566, 1975.

[12] Gibson, M.M. and Launder, B.E. *Ground effects on pressure fluctuations in the atmospheric boundary layer*. J. Fluid Mech., Vol. 86(03), pp. 491-511, 1978.

[13] Pope, S.B. *Turbulent Flows*. Cambridge University Press, 2000.